IAHR AIRH
Taylor & Francis
Taylor & Francis Group

Journal of Hydraulic Research Vol. 48, No. 1 (2010), pp. 14–22
doi:10.1080/00221680903565879

Research paper

Mechanism of rock-bed scour due to impinging jet

AIHUA LI, *College of Petroleum Engineering, China University of Petroleum, Dongying, Shandong 257061, People's Republic of China.*
Email: aiwali0524@163.com (author for correspondence)

PEIQING LIU (IAHR Member), *School of Aeronautical Science and Engineering, Beihang University, Beijing 100083, People's Republic of China.*
Email: bhlpq@263.net

ABSTRACT
Scour of rock bed downstream of high dams is mainly caused by the transient forces as a result of the propagation of fluctuating pressures, which is significan controlled by the rock fracture-structure. The physical mechanism of rock disintegration and scour pool forming are analysed herein by considering the fra ture-structure of rock bed. A two-dimensional discrete fracture network is imitated applying the Monte-Carlo method. The model of transient flow is esta lished along with each discrete fracture to simulate numerically the propagation of fluctuating pressure waves. Applying the method of automatic tracing rock blocks layer by layer, the mechanism of disorganization of fractured rock, both the transient physical and dynamic characteristics of isolated rocks, and t damage process of the rock bed are discussed. Finally, a stability criterion of rock blocks and the evaluation method of equilibrium scour depth are establish

Keywords: Discrete fracture network, fluctuating pressure, jet, Monte-Carlo method, rock scour

1 Introduction

The dislodgement of lining slabs over river beds, and the formation and development of scour pools downstream of high dams are caused by the propagation of fluctuating pressures within the rock fissures (Bowers and Toso 1988, Fiorotto and Rinaldo 1990, Annandale 2006, Manso 2006). Bellin and Fiorotto (1995), and Fiorotto and Rinaldo (1990, 1992a, 1992b) proposed the transient model to account for the propagation mechanism of fluctuating pressure, based on the pressure transient characteristics within joints. Bollaert (2002) and Bollaert and Schleiss (2003, 2005) studied the effect of air entrained in the water and proposed the two-phase transient hydraulic model.

In laboratories, fissured rock bed is considered as a continuous medium (Hanson *et al.* 1998). In fact, there exist many faults, fissures and cracks in bedrock, allowing for passage of water flow. The "homogeneous" model cannot reflect the actual fissure distribution and the flow characters in it, and may lead to mistakes (Mason and Arumugam 1985, Stein *et al.* 1993). Johnson (1977) proposed that especially the sharp steps contained in actual scour cannot be exactly reproduced by applying (semi-)empirical formulas.

The particular structural character of bedrock, such as its density, spatial distribution, coarseness, stretch degree and filling degree of the fractures determine largely the fluctuating pressure propagatio Ouenes (2000) attempted to characterize natural fractures by appl ing fuzzy logic and neural networks. This method is not direct applicable for the present research, however, requiring simulati and treatment of physical fractures inside the rock. Based on t statistics, probability theory and the fractal geometry, Hammersl and Handsconmb (1964) and Chen (2001) proposed a thre dimensional network simulation technique, namely the Mont Carlo method, which has been applied widely in the seepage fiel

The discrete fracture network (DFN) is generated herein by appl ing the Monte-Carlo method and introducing a numerical study hydraulic scour downstream of high dams. The transient proce of fluctuating pressures within each fissures and the spatial streng distribution of pressure fluctuating within the network are simulate Applying statistical theory, the propagation mechanism of fluctua ing pressures within the complex fracture network is analysed.

2 Generation of DFN

2.1 *Monte-Carlo simulation*

Simulation of DFN is a complex procedure of generating nume ous fractures in a block of rock processing geologic, geophysic

Revision received 2 November 2009/Open for discussion until 31 August 2010.

ISSN 0022-1686 print/ISSN 1814-2079 online
http://www.informaworld.com

engineering data so that the generated fractures are con-ned to represent the prototype fractures. The Monte-Carlo hod is a process including field test, statistical analysis of fracture characteristics, random numbers for each fracture racteristic generation according to its distribution map and ture networks statistically equivalent to the generated proto- natural facture networks.

For simulating a two-dimensional (2D) DFN by the fractal cept, a square longitudinal section of 10 m × 10 m is con-red. The jth with $j = 1, 2, 3, \ldots, j_{\max}$ fracture is defined by centre position O_j (x, y), the dip angle α_j and the fracture gth L_j, where $j_{\max}$ is the fracture total. Each fracture has two es, the jth fracture being between nodes i and $i + 1$. The e total is $i_{\max}$. The network discontinuity density is the reci-cal of the mean distance between the fractures. These are gen-ly distributed uniformly in rock, the fracture centre $O_j(x, y)$ ng defined by generating uniform random numbers between nd 1 in two directions. Natural fractures are commonly ped in a preferred degree α_j obeying the normal distribution, the fracture length L_j obeys a negative exponential distri-ion and the log-normal distribution. According to the speci- ranges and the prototype distributions observed, α_j and L_j sampled randomly in uniform random numbers between 0 1 using the inverse function method. If the density simulated ees with the prototype data, the network simulation is shed. Applying the Monte-Carlo method, a 2D DFN was ulated using a FORTRAN program (Table 1, Fig. 1). A t matrix and a loop matrix explain the DFN.

The correlation between fracture nodes and cells is defined as joint matrix $\mathbf{A} = \{a_{ij}\}$

$$a_{ij} = l_j \ (i = 1, \ j = 2 \sim j_{\max} + 1) \tag{1}$$

$$a_{ij} = m_i \ (j = 1, \ i = 2 \sim i_{\max} + 1) \tag{2}$$

$$a_{ij} = \begin{cases} 0, & \text{cell } l_j \text{ does not join node } m_i \\ +1, & \text{cell } l_j \text{ joins node } m_i \text{ and deviates from it} \\ -1, & \text{cell } l_j \text{ joins node } m_i \text{ and points to it} \end{cases} \quad \begin{pmatrix} i = 2 \sim i_{\max} + 1 \\ j = 2 \sim j_{\max} + 1 \end{pmatrix} \tag{3}$$

le 1 Statistical distribution of rock fracture characteristics

cture racteristics	Distribution	Group I	Group II
an fractural istance		1 m	1.25 m
sity	Uniform	1 m^{-1}	0.8 m^{-1}
angle α_j	Normal	AVER(α_j) = 60° SQRT(α_j) = 2°	AVER(α_j) = −60° SQRT(α_j) = 2°
gth L_j	Negative exponential	AVER(L_j) = 7 m	AVER(L_j) = 10 m

e: AVER, statistic mean value; SQRT, standard deviation value.

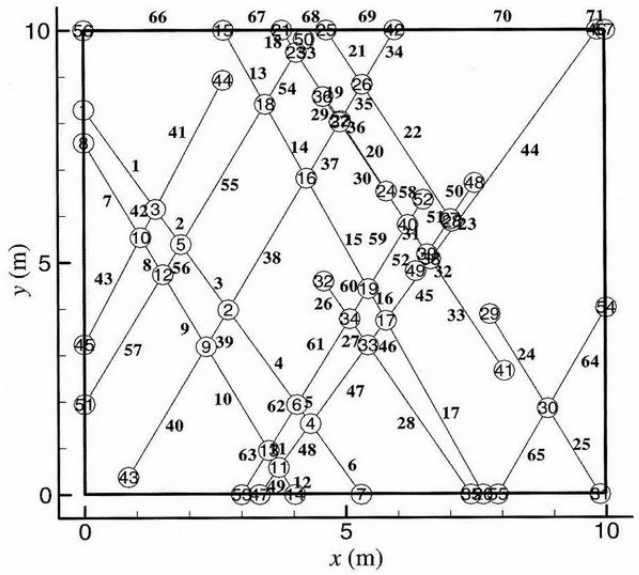

Figure 1 Sketch of imitated fracture network

The basic loop within a fracture network is defined as loop matrix $\mathbf{L} = \{L_{kj}\}$

$$L_{kj} = \begin{cases} 0, & \text{cell } l_j \text{ is not included in loop } k \\ +1, & \text{cell } l_j \text{ is included in loop } k \text{ and with the same direction} \\ -1, & \text{cell } l_j \text{ is included in loop } k \text{ and with the reverse direction} \end{cases} \tag{4}$$

2.2 *Automatic tracing of isolated rock block*

The automatic tracing of isolated rock block allows one to seek a basic loop within the rock mass (Fig. 2):

(1) *Chop tree:* delete the cells that have no intersections or have only one with others;
(2) Define clockwise as positive direction of each loop. Select S_1 as the basic cell and A_1 as the basic forward node;
(3) Seek any other cells intersecting with S_1 at A_1, such as R_2, R_2', R_2'' etc. Pick one that has the smallest anticlockwise angle from S_1 and mark it as S_2, and the forward node of S_2 is A_2;
(4) Similarly, continue in circle until the loop is closed. Then the traced loop defines the smallest block within the rock mass.

When the key blocks on the surface are pulled up and taken away due to hydrodynamic pressure, other adjacent blocks are easily dislodged. After the surface damage, the new surface blocks are traced by applying the automatic tracing method of isolated blocks.

3 Numerical simulation of pressures propagation

3.1 *Transient model*

If a high-speed jet is discharged from a high arc dam, the upper rock boundary is exposed to intense pressure fluctuations. Based

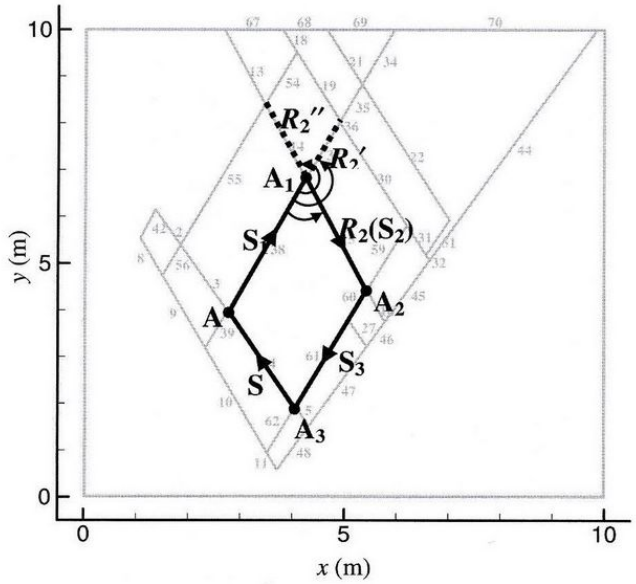

Figure 2 Tracing of isolated rock block

on the transient and wave characteristics of pressure propagation within slab joints, Fiorotto and Rinaldo (1992a, 1992b) regarded the pressure propagation as a process of hydrodynamic transient. Liu and Li (2007) discussed the model of pressure propagation and proposed the uniform transient model. Within the imitated fracture network, a 1D transient model was established along with each fracture cell as

$$\frac{\partial u}{\partial t} + u\frac{\partial u}{\partial x} + g\frac{\partial u}{\partial x} + R(u)u = 0 \tag{5}$$

$$\frac{\partial h}{\partial t} + u\frac{\partial h}{\partial x} + \frac{a^2}{g}\frac{\partial u}{\partial x} = 0 \tag{6}$$

where x is the streamwise coordinate, a the pressure wave celerity, $h = p'/\gamma$ the fluctuating pressure head p', $\gamma = \rho g$ the specific weight of water, ρ the water density, g the acceleration due to gravity and u the average velocity within the fissure due to the fluctuating pressure. $R(u) = \lambda|u|/4\delta$ = drag term, where δ is the thickness of fissure and λ the dimensionless blockage coefficient proportional to the joint roughness coefficient with a complex relation to the filling material and degree in the fissure.

Fiorotto and Rinaldo (1990) observed that the drag effect determines pressure propagation for very narrow fractures. Liu and Li (2007) discussed the drag term using theoretical analysis and numerical simulation, and deduced that the drag term significantly attenuates the high-frequency proportion of fluctuating pressures. Bollaert (2002) proposed that the air entrained in the impinging jet may significantly reduce the propagation velocity and may lead to pressure resonance. All these effects complicate the problem. Because the main purpose herein is the methodological study of rock scour, the following assumptions are made:

(1) Drag term effect on pressure transfer is neglected.
(2) Influence of air entrained is not considered.
(3) Propagating velocity of pressure wave is assu a=1000 m/s.
(4) Impinging jet is fully developed.

At the initial moment, $t = 0$, $h = 0$ and $v = 0$. The bo boundary of the control volume is assumed impermea whereas the left and right boundaries are permeable. Unde impingement, the severe fluctuating pressures acting on upper boundary generally obey the normal distribution have the low Eigen-frequency of less than 10 Hz (Cui 1 Liu 1994, Liu and Li 2007). The second-order terms neglected and the characteristic method is applied. The step is $\Delta t = 0.001$ s, the spatial step is $\Delta l = a \cdot \Delta t = 1$ m the total calculating time is 10 s.

3.2 *Distribution of fluctuating pressures*

During impact of a water jet downstream of a high dam, the s depth gradually increases. Figure 3 shows a sketch of dynamic rock bed under jet impingement.

At a certain time, u_o is the jet velocity, d_o the jet thickne the jet impact angle, h_o the water depth, h_t the depth of scour and s the initial impinging point. At initial scour depth h_o coordinates are (x, y) with the origin O. The intersection o jet centreline and the dynamic rock bed is the dynamic impin point s'. The vertical line from point s' intersects the w surface at point O′, selected as the origin of the dynamic coo nate system (x, y'). The corresponding coordinates of any poi on the dynamic rock bed is (x_w, y_w').

The maximum pressure fluctuation and the time-avera pressure are located close to the jet impact point. The r mean-square (RMS) pressure fluctuation σ at s is (Cui e 1982)

$$\sigma_s = \frac{1}{2}\rho u_o^2 \cdot 0.5\mathrm{e}^{-0.0265(h_o/d_o)^{1.14}} \cdot \sin^2\beta$$

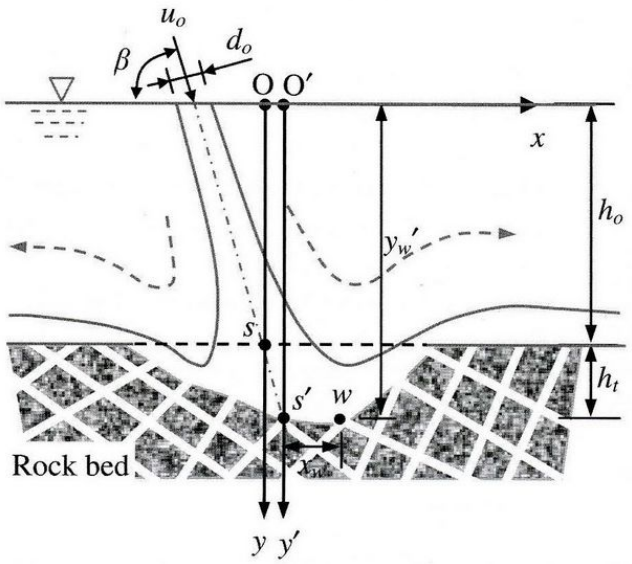

Figure 3 Sketch of dynamic rock bed under jet impingement

As the scour depth increases, the energy carried in the jet is gradually dissipated in the scour pool. If $y = y_w$, the RMS pressure fluctuation at point s' is

$$\sigma_{s'} = \frac{1}{2}\rho u_o^2 \cdot 0.5\mathrm{e}^{-0.0265(h_o+h_t/d_o)^{1.14}} \cdot \sin^2\beta \left(\frac{h_o}{d_o} > 13\right) \quad (8)$$

And the correlation between the RMS of any points w and s' is determined by

$$\sigma_w = \sigma_{s'} \cdot \mathrm{e}^{-6.25X^{1.4}} = \frac{1}{2}\rho u_o^2 \cdot 0.5\mathrm{e}^{-0.0265(h_o+h_t/d_o)^{1.14}-6.25X^{1.4}} \cdot \sin^2\beta \quad (9)$$

where the relative distance of point w to s' is $X = x_w/h_{co}$ for $x > 0$, and $X = |x_w|/r'h_{co}$ for $x < 0$. Further, the efficient water depth follows from

$$\frac{h_{co}}{h_o} = \left\{1 - 2\mathrm{F}_c\left[\left(\frac{u_o}{u_c}\right)\theta(1+\cos\beta) - 1\right]\right\}^{1/2} \quad (10)$$

where $\theta = 0.6$, $r' = (\sin\beta - 0.1\cos\beta)/(\sin\beta + 0.1\cos\beta)$ the asymmetric jet coefficient, u_c the critical velocity, and $\mathrm{F}_c = u_c/(gh_o)^{0.5}$ the critical Froude number.

Using the specific parameter σ_s, Eq. (10) can be normalized to

$$\frac{\sigma_w}{\sigma_s} = \mathrm{e}^{0.0265[(h_o/d_o)^{1.14} - (h_o+h_t/d_o)^{1.14}]-6.25X^{1.4}} \quad (11)$$

From Eqs (9) and (11), the fluctuating pressure intensity at any point w of the dynamic rock bed decreases as h_0 and the relative distance X from s' increase. To simulate pressure propagation within the imitated rock fracture network, the first fissure node from left to right on the initial rock plane is supposed to be s. The fluctuating pressure wave acting on w is therefore

$$h_w = \frac{\sigma_w}{\gamma} \cdot q(t) \quad (12)$$

where h_w is the numerically imitated fluctuating pressure wave, following the normal distribution $N(\mu, \sigma)$ with low Eigen-frequency, where, $\mu = 0$ and $\sigma = \sigma_w$ are the mean and RMS values of the fluctuating pressure, respectively. σ_w is determined according to Eqs (9) or (11); $q(t)$ is a stochastic process, obeying the standard normal distribution $N(0, 1)$. Here, $q(t)$ is constructed by 40 sine and cosine functions with different frequencies and amplitudes, to assure that the main frequency of the pressure wave is smaller than 10 Hz. Figure 4 shows $q(t)$ and its spectrum curve, respectively.

3.3 *Results of numerical simulation*

The temporal process and statistical characteristics of fluctuating pressures propagation within each fissure, and the special distribution of pressure intensity fluctuations are determined using numerical simulation. Figure 5 shows the spatial distribution of the relative RMS to σ_s. Figure 6 shows the time process and the spectrum curve of point k marked in Fig. 5.

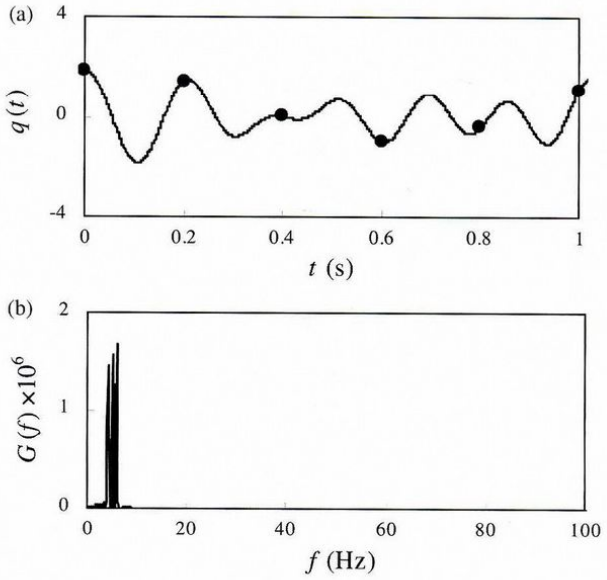

Figure 4 (a) Time process curve of $q(t)$; (b) spectrum curve

From Figs 5 and 6, it can be concluded that the fluctuating pressure propagation within the fracture network is a complex process. The pressure wave within any fracture differs from that at s is represented by $q(t)$ ($q(t) = p_s'/\sigma_s$), made up of many high-frequency fluctuations. The fluctuating pressure of any node within the network is a summation of pressure waves propagated in it and the reflected waves from any other adjacent fissures. The reasons are as follows:

(1) The fluctuating pressure propagation within the fracture network has typically anisotropic characteristics. The equivalent continuum models do not adapt to rock scour. Applying the fracture network explains more accurately this phenomenon.

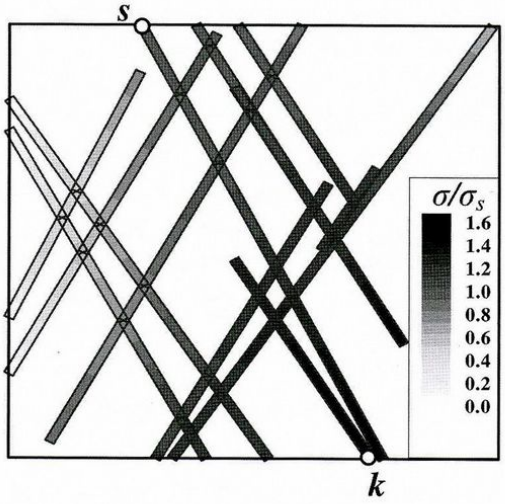

Figure 5 Spatial distribution of RMS

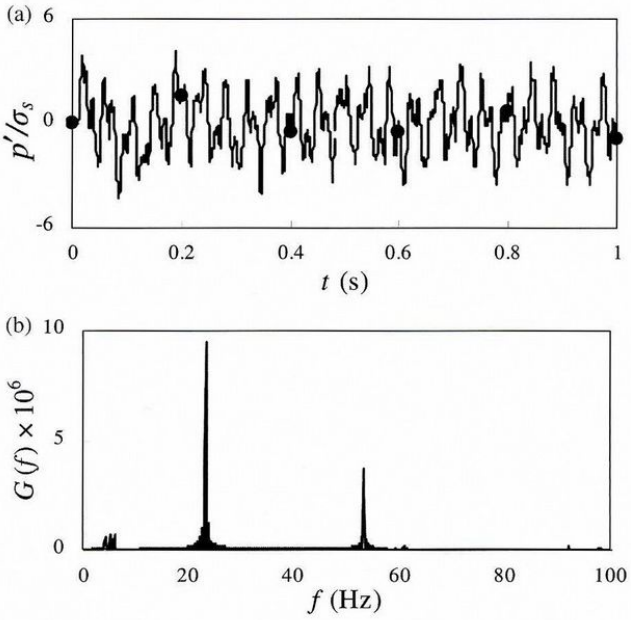

Figure 6 (a) Time process curve of p'/σ_s; (b) spectrum curve

(2) The pressure fluctuations remarkably amplify within fissures. The computational results indicate that the maximum RMS within the fracture networks can reach up to $1.639\sigma_s$, whereas the maximum of p' can reach $4.3\sigma_s$. Especially at the closed fissure ends, a concentrated zone of hydrodynamic stress occurs, promoting the fissured rock to be wedged by the jet and to be further fractured.

4 Mechanisms of rock disintegration and scour pool formation

4.1 *Scour process*

Under high-velocity jet impact, scouring is a physical process involving (1) impinging jet generating intense pressure fluctuations acting on fissured bed, (2) fluctuating pressures propagating rapidly within the fractures, (3) propagation of fissures into rock resulting in rock bed disintegration, (4) isolated rock blocks vibrating randomly and being dislodged ultimately, (5) rock bed scour layer by layer and (6) scour pool reaching equilibrium depth (Fig. 7). The first two items were considered above and the others follow below.

4.2 *Disintegration of rock bed*

Based on the theory of spread and crash of fractures, the crash of rock bed mainly experiences two stages, i.e. generation and spread of fractures. Because many initial micro-fractures are involved in prototype rock, new fractures are generated as the water jet impacts a concentrated zone of alternative stress at the top fracture ends if the stress exceeds the limited intensity of rock crash. Simultaneously, the initial micro-fractures spread and develop rapidly along with their own crack line. Along with the continuous transfer of jet dynamic energy, the fractures

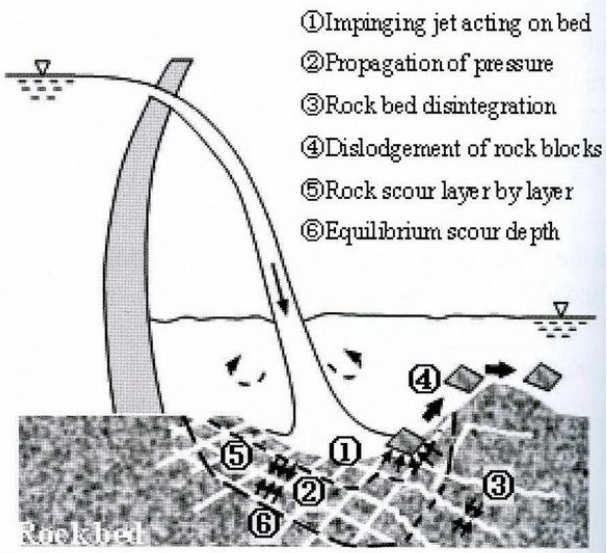

Figure 7 Physical model of rock scour.

then penetrate through the rock crystal boundaries spreadin intersecting gradually. Finally, the whole rock bed is com of many cracked rock blocks of different dimensions and ent shapes.

4.3 *Dislodgement of isolated rock blocks*

The float stability of rock blocks is one of the main crite rock scour damage. The forces acting on an isolated block include stable forces and uplift forces. The stable f include gravity $G = \rho_r V_r g$, where V_r is the rock volume, rock density, where $\rho_r = 2.7 \sim 2.8 \times 10^3$ kg/m^3 for the rock, shear resistant force F_τ and the drag resistant forc The uplift forces include the fluctuating pressures within tures P', decomposed to vertical P'_v and horizontal P'_h, the fl ating pressure on the rock surface P'_u and the time-aver hydro-dynamic pressure $\rho V_r g$. These are all unit-width f (Fig. 8). To assure vertical rock block stability,

$$P'_v + P'_u + \rho V_r g = \rho_r V_r g + F_R + F_\tau$$

For the block shown in Fig. 8, the fluctuating pressu within fracture j is

$$P'_j = \gamma \sum_{m=1}^{n-1} h_{jm} \cdot \Delta l_j$$

Considering the three surrounding fracture cells (i.e. $j =$ the dip angle α_j, P'_v and P'_h for each cell, the resultant force

$$P'_{vj} = P'_j \cdot (\pm \cos \alpha_j), \quad P'_v = \sum_{j=1}^{3} P'_{vj}$$

$$P'_{hj} = P'_j \cdot (\pm \sin \alpha_j), \quad P'_h = \sum_{j=1}^{3} P'_{hj}$$

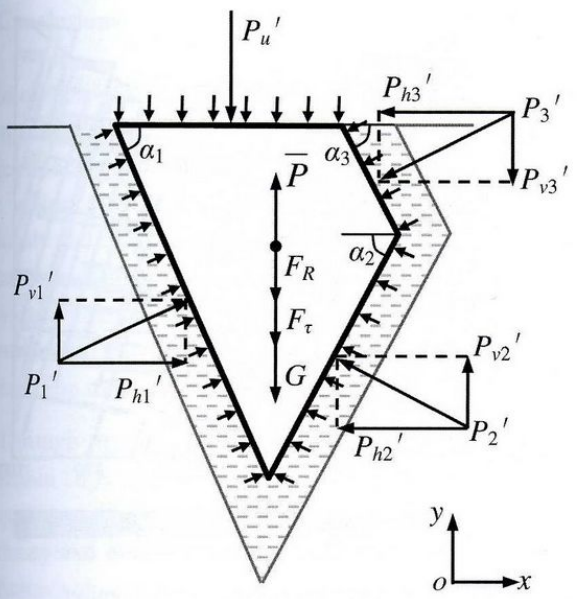

Figure 8 Dynamic block characteristics

The fluctuating pressure P' acting on the isolated block thus is

$$P' = \sqrt{P_v'^2 + P_h'^2} \tag{17}$$

If $\Delta l = 1$ m, and if two fissures have a distance of less than 1 m, the fluctuating pressures are strongly correlated to each other and the pressure force P' acting on the isolated rock block tends to zero. Such small blocks are assumed to be destroyed here.

Figure 9 shows the time process curve of the vertical fluctuating pressure P_v' and the horizontal fluctuating pressure P_h' acting on a given block using $\sigma_s D$, with $D = (4S/\pi)^{0.5} = 1.23$ m as the equivalent rock block diameter and S the rock area. It was observed that intense vertical fluctuating pressure promotes block dislodgement. The horizontal fluctuating pressure prompts the block being relaxed and shaken, which also promotes the dislodgement. Moreover, P_u' is determined with the boundary conditions under jet impingement. Cui (1986) recommends $P_u' = \pm 3\sigma_s$. Assuming $P_v' + P_u' = f_1(\sigma_s)$, the stability criterion of rock block is

$$f_1(\sigma_s) < (\rho_r - \rho)V_r g + F_R + F_\tau \tag{18}$$

$$\sigma_s < f_1^{-1}\left[(\rho_r - \rho)V_r g + F_R + F_\tau\right] \tag{19}$$

Once the function $f_1(\sigma_s)$ is established via numerical simulation, the rock bed stability can be analysed quantitatively. For different blocks, the hydraulic conditions and the structural characters differ, and so the functions $f_1(\sigma_s)$ are different too.

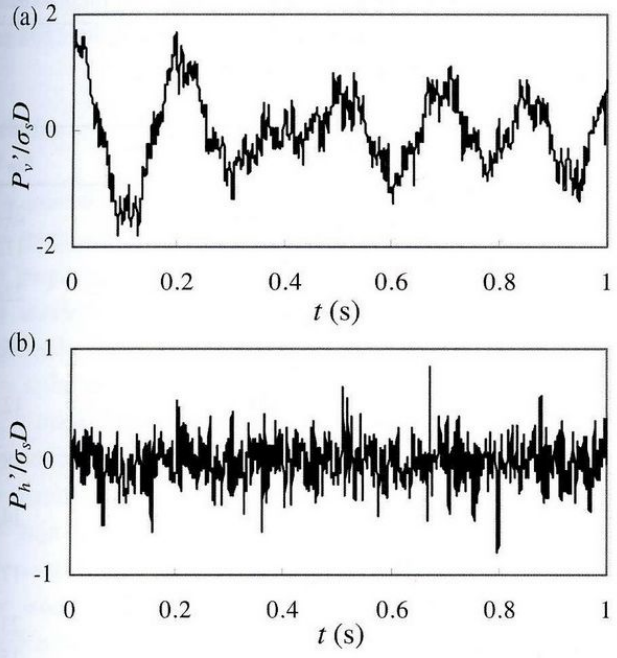

Figure 9 (a) Vertical fluctuating pressure P_v'; (b) horizontal fluctuating pressure P_h'

4.4 *Rock scour layer by layer and equilibrium scour depth*

Rock scour is a process of isolated blocks dislodged layer by layer. If the surface isolated blocks do not meet the stability criterion after Eq. (19), they will be dislodged at a certain time resulting in a new surface. The dynamic characteristics and the stability of the isolated blocks on the new surface must then be re-analysed and repeated until all surface-isolated blocks meet the stability criterion and reach the equilibrium scour depth. Figure 10 shows the simulated dynamic rock bed at the first four damage stages.

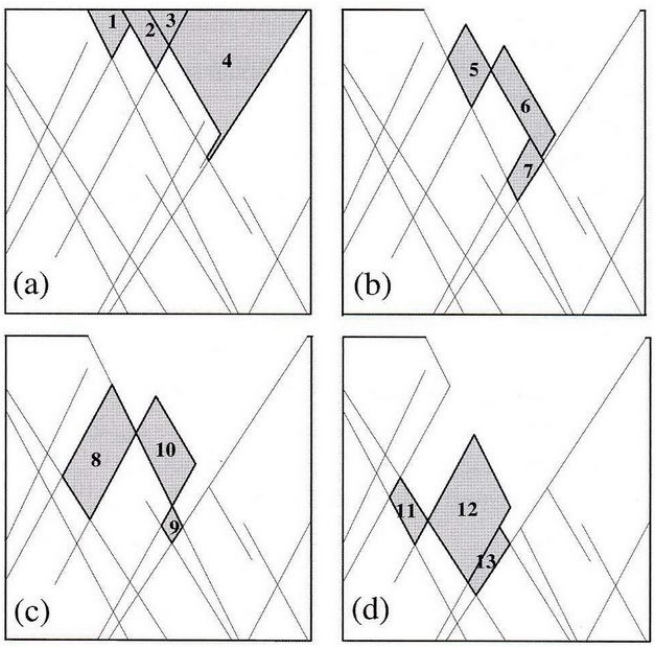

Figure 10 Stages (a) I, (b) II, (c) III, (4) IV

Table 2 Statistics of rock fractures on right bank

Testcave	Fracture groups	Fracture numbers	Strike angle (°)	Dip angle (°)		Fracture length (m)	
				AVER	SQRT	AVER	SQRT
D07	1	38	191.1	71.5	0.02	100	0.237
	2	26	2.3	8.5	0.03	100	0.662

5 Scour prediction of Xi Luo Du hydro-electric plant

The Xi Luo Du hydro-electric power plant is located at the Jing Sha River in China. The rock scour downstream of the high-arc dam is simulated below, introducing the DFN as follows:

(1) Based on site data in Cave D07 (Table 2), DFN is imitated from 70 to190 m downstream from the dam toe, reaching a depth of 100 m.
(2) Two fracture groups are uniformly distributed with the density of 0.8 m^{-1}. Assume the rock bed totally cracked, and the mean length and thickness of fractures are 100 m and 2 mm, respectively.
(3) The up- and downstream boundaries are permeable whereas the bottom is impermeable. The site conditions are listed in Table 3.

Figure 11 shows the numerical result of the equilibrium scour pool by a real line and the spatial distribution of the relative RMS to σ_s, the mean scour curve is also given by the dotted line. For

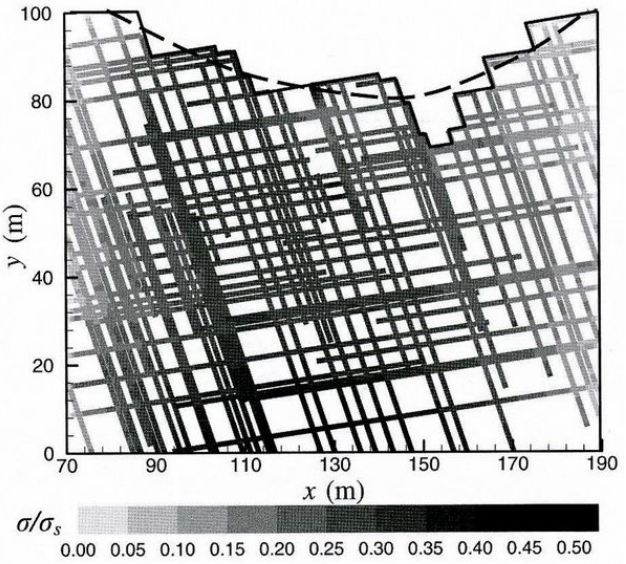

Figure 11 Equilibrium scour pool of Xi Luo Du project

these conditions, the ultimate scour depth is about 31 m, the scour pool is stretched downstream about 104 m (fro to 190 m).

The Monte-Carlo method is a random statistical met Three different networks were simulated in addition to c lation of the mean value of maximum scour depth. Table 4 pares the scour depth predictions with other (semi-)empi formulations. Obviously, the predicted results by nume simulation using DFN compare well with the (semi-)empi results.

Table 3 Overflow conditions of #5 surface opening

Upstream water level Z_u (m)	Downstream water level Z_d (m)	Unit-width discharge q (m^2/s)	Jet impact velocity u_o (m/s)	Jet impact thickness d_o (m)	Jet impact degree β (°)	Trajectory jet distance L_o (m)	Cushi depth h_c
603.98	410.31	99.396	58.231	18.511	72.08	116.19	28.8

Table 4 Prediction comparison of equilibrium scour depth

Formulations (Liu 1994)		h_m (m)	h_t
Damle (C)	$h_m = 0.362 \cdot q^{0.5}(Z_u - Z_d)^{0.5}$	50.23	2
Martins (B)	$h_m = 1.5 \cdot q^{0.6}(Z_u - Z_d)^{0.1}$	40.11	1
Taraimovich	$h_m = 0.663 \cdot q^{0.67}(Z_u - Z_d)^{0.25}$	51.45	2
Mason	$h_m = 3.27\dfrac{q^{0.6}(Z_u - Z_d)^{0.05}h_o^{0.15}}{g^{0.3}D^{0.1}}$	54.85	2
Chen	$h_m = 1.1q^{0.5}(Z_u - Z_d)^{0.25}$	40.91	1
Yu	$h_m = 1.172\dfrac{q^{0.75}(Z_u - Z_d)^{0.125}}{1.9}$	37.50	
Liu	$h_m = 0.74 \cdot (0.41 + 0.082D)\dfrac{q^{2/3}(Z_u - Z_d)^{1/3}}{d^{1/3}}$	43.70	1
Liu	$h_m = \sqrt{h_o^2 + K_T^2\dfrac{q\sqrt{Z_u - Z_d}}{\sqrt{g}}}\quad K_T^2 = 6.76\left(\dfrac{d_o \sin\beta}{h_m}\right)^{0.5}$	46.76	1
Numerical mean results	Real (full line)	52.56	2
	Average (dotted line)	44.56	1

Note: $D = 1.25$ m the average special diameter of rock blocks

Conclusions

cour of rock bed is a sequential dynamic process of rock being isorganized, fragmentized and dislodged. During rock scour, ıe jet flow character, the structure of rock mass and the stress ate within the network are all changed momentarily. It is bviously deficient to study pressure propagation, which has pical anisotropic character, based on the static theory and the quivalent continuum models. A complex rock fracture etwork was introduced herein to simulate the rock scour rocess. The main conclusions include:

1) Through numerical simulation of pressure propagation within DFN, the development of the scour hole is described quantitatively and visually. The scour hole shape, depth and the spatial distribution of pressure fluctuations within rock fissures at each stage are obtained.
2) The general model of rock scour, i.e. jet impinging, propagation of fluctuating pressures, rock disintegration, isolated rock dislodgement, layer by layer rock bed scour, and equilibrium scour depth, is described.
3) Applying numerical simulation to predict rock scour downstream of Xi Luo Du hydro-electric power plant provides reasonable simulation results.

FN may be considered a breakthrough of rock scour simuıtion, despite many aspects were not considered due to comlexity, including the effects of jet aeration, resonance, drag in ressure propagation and lateral confinement of scour hole, otential of brittle fracture or fatigue failure.

cknowledgements

his research has been financially supported by the National latural Science Foundation of China, Grants Nos. 10772015 nd 50539060.

otation

= joint matrix
= propagating velocity
= frequency of fluctuating pressure
= acceleration due to gravity
= head of fluctuating pressure
= scour depth
$_m$ = maximum scour depth
= number index of fracture node
= number index of fracture cell
= index of network loop
= loop matrix
= length of fracture cell j
= time-averaged pressure
= fluctuating pressure
= jet impact point
α_j = dip angle of fracture cell j
γ = specific weight of water
δ = thickness of fissure
λ = dimensionless joint blockage coefficient
ρ = water density
ρ_r = rock density
σ = standard deviation of pressure fluctuation

References

Annandale, G.W. (2006). *Scour technology.* McGraw-Hill, New York.

Bellin, A., Fiorotto, V. (1995). Direct dynamic force measurement on slabs in spillway stilling basins. *J. Hydraul. Eng.* 121(10), 686–693.

Bollaert, E. (2002). The influence of plunge pool air entrainment on the presence of free air in rock joints. Proc. Intl. Workshop. *Rock Scour Due to High-velocity Jets*. EPFL Lausanne, Switzerland, 137–149.

Bollaert, E., Schleiss, A. (2003). Scour of rock due to the impact of plunging high velocity jets 1: Experimental results of dynamic pressures at pool bottoms and in one- and two-dimensional closed end rock joints. *J. Hydraulic Res.* 41(5), 465–480.

Bollaert, E., Schleiss, A. (2005). Physically-based model for evaluation of rock scour due to high velocity jet impact. *J. Hydraul. Eng.* 131(3), 153–165.

Bowers, C.E., Toso, J. (1988). Karnafuli project, model studies of spillway damage. *J. Hydraul. Eng.* 114(5), 469–483.

Chen, J.P. (2001). 3-D network numerical modeling technique for random discontinuities of rock mass. *J. Geotech. Eng.* 23(4), 397–402, [in Chinese].

Cui, G.T. (1986). Discussion of the maximum breadth of water fluctuating pressure. *Information net of high-speed flow.* 2nd Congressional Corpus, Beijing, China 10, 84–88, [in Chinese].

Cui, G.T., Lu, R.G., Lin, J.Y. (1982). Discussion to dynamic pressures due to ski-jump jet and protection of rock bed. *J. Tian Univ.* 2, 23–26, [in Chinese].

Fiorotto, V., Rinaldo, A. (1990). Discussion to Karnafuli project, model studies of spillway damage. *J. Hydraul. Eng.* 116(6), 850–852.

Fiorotto, V., Rinaldo, A. (1992a). Fluctuating uplift and lining design in spillway stilling basins. *J. Hydraul. Eng.* 118(4), 578–596.

Fiorotto, V., Rinaldo, A. (1992b). Turbulent pressure fluctuations under hydraulic jumps. *J. Hydraulic Res.* 30(4), 499–520.

Hammersley, J.M., Handsconmb, S.C. (1964). *Monte-Carlo method.* Methuen, London.

Hanson, G.J., Robinson, K.M., Cook, K.R. (1998). Erosion of structured material due to impinging jet. Proc. Intl. *Water*

Resources Engineering Conference. Memphis, TN, ASCE, New York, 1102–1107.

Johnson, G.M. (1977). Use of a weakly cohesive material for scale model scour studies in flood spillway design. 17th *IAHR Congress*. Baden-Baden, 4(C63), 509–512.

Liu, P.Q. (1994). Mechanism of free jet's scour on rocky riverbeds. *PhD thesis*. Higher Education Press, Beijing, China, [in Chinese].

Liu, P.Q., Li, A.H. (2007). Model discussion of pressure fluctuations propagation within lining slab joints in stilling basins. *J. Hydraul. Eng*. 133(6), 618–624.

Manso, P.A. (2006). The influence of pool geometry and induc flow patterns on rock scour by high-velocity plunging je *PhD thesis*, EPFL, Lausanne, 3430.

Mason, P.J., Arumugam, K. (1985). Free jet scour below dar and flip buckets. *J. Hydraul. Eng*. 111(2), 220–235.

Ouenes, A. (2000). Practical application of fuzzy logic a neural networks to fractured reservoir characterizatic *Comput. Geosci*. 26(8), 953–962.

Stein, O.R., Julien, P.Y., Alonso, C.V. (1993). Mechanics of scour downstream of a headcut. *J. Hydraulic Res*. 31(723–738.